

---

# $S_0$ Tuning: Zero-Overhead Adaptation of Hybrid Recurrent-Attention Models

---

**Jack Young**  
Independent Researcher  
jackhyoung@gmail.com

## Abstract

Using roughly 48 execution-verified HumanEval training solutions, tuning a single initial state matrix per recurrent layer, with zero inference overhead, outperforms LoRA by +10.8 pp ( $p < 0.001$ ) on HumanEval. The method, which we call  $S_0$  tuning, optimizes one state matrix per recurrent layer while freezing all model weights. On Qwen3.5-4B (GatedDeltaNet hybrid),  $S_0$  tuning improves greedy pass@1 by +23.6  $\pm$  1.7 pp (10 seeds). On FalconH1-7B (Mamba-2 hybrid),  $S_0$  reaches 71.8%  $\pm$  1.3 and LoRA reaches 71.4%  $\pm$  2.4 (3 seeds), statistically indistinguishable at this sample size while requiring no weight merging. Cross-domain transfer is significant on MATH-500 (+4.8 pp,  $p = 0.00002$ , 8 seeds) and GSM8K (+2.8 pp,  $p = 0.0003$ , 10 seeds); a text-to-SQL benchmark (Spider) shows no transfer, consistent with the trajectory-steering mechanism. A prefix-tuning control on a pure Transformer (Qwen2.5-3B) *degrades* performance by -13.9 pp under all nine configurations tested. On Qwen3.5, a per-step state-offset variant reaches +27.1 pp, above both  $S_0$  and LoRA but with per-step inference cost. Taken together, the results show that recurrent state initialization is a strong zero-inference-overhead PEFT surface for hybrid language models when verified supervision is scarce. The tuned state is a ~48 MB file; task switching requires no weight merging or model reload. Code and library: <https://github.com/jackyoung27/s0-tuning>.

## 1 Introduction

Production language models increasingly combine recurrent layers with standard attention in a single backbone Yang et al. [2024], Dao and Gu [2024], Falcon LLM Team [2025]. The recurrent component varies. Qwen3.5 interleaves three GatedDeltaNet layers per attention layer; FalconH1 places Mamba-2 and attention heads in parallel within each layer. These hybrid architectures achieve subquadratic sequence cost while retaining the in-context learning of full attention. They also expose a new adaptation surface that pure Transformers lack: the recurrent hidden state  $S_t$ , a matrix updated at every token.

LoRA Hu et al. [2021] and its descendants adapt weight matrices, a strategy introduced for and validated on Transformers. Hybrid models, however, carry a per-layer state matrix that accumulates distributional information across the entire context window and is set to zero by default. Replacing that zero with a learned value steers the model toward a target task.

Hybrid recurrent-attention backbones now ship in major open-weight releases Yang et al. [2024], Falcon LLM Team [2025], Lahoti et al. [2026], yet PEFT has not kept pace: LoRA and prefix tuning target weight matrices and leave the recurrent state at its default zero.  $S_0$  tuning optimizes a single state matrix  $S_0$  per recurrent layer (12.6M parameters, 0.3% of Qwen3.5-4B) with all weights frozen. On HumanEval, this improves greedy pass@1 by +23.6  $\pm$  1.7 pp, outperforming LoRA by +10.8 pp ( $p < 0.001$ , 10 seeds each) with zero inference overhead. On FalconH1-7B, a Mamba-2 hybrid with a fundamentally different recurrence family,  $S_0$  reaches 71.8%  $\pm$  1.3 and LoRA reaches 71.4%  $\pm$  2.4

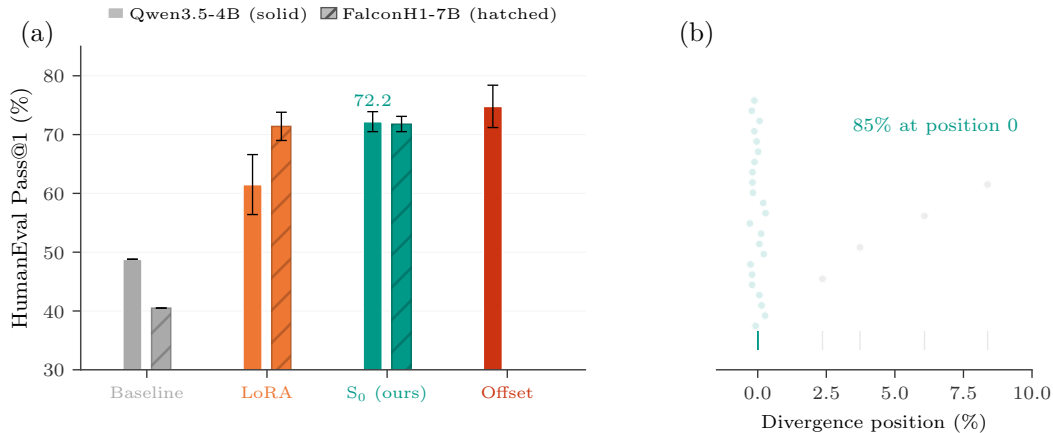


**Figure 1: Overview of  $S_0$  tuning.** (a) Cross-architecture comparison on HumanEval:  $S_0$  (teal) outperforms LoRA on Qwen3.5-4B and is tied with it on FalconH1-7B (hatched bars). The Qwen comparison is significant ( $p < 0.001$ ; \*\*\*); the Falcon 3-seed comparison is statistically indistinguishable from LoRA. Offset is shown for Qwen only (not applicable to FalconH1’s recurrence). Error bars show  $\pm 1$  std across seeds. (b) First-character divergence: of 27 FAIL-to-PASS flips, 23 (85%) diverge from baseline at the very first generated character (teal dots at position 0).

(3 seeds each), statistically indistinguishable at this sample size. Prefix tuning applied to a pure Transformer (Qwen2.5-3B) degrades performance by  $-13.9$  pp under all nine configurations tested.

This is a small-data paper. Roughly 48 verified HumanEval solutions move Qwen3.5-4B by  $+23.6$  pp and beat LoRA by  $+10.8$  pp over 10 seeds; Falcon supplies a 3-seed second architecture at 71.8% versus 71.4% for LoRA, and the math benchmarks add smaller but significant gains. That is enough to establish the main point: recurrent state is a high-leverage adaptation surface for hybrid models, while the remaining experiments map transfer, scale, and failure modes.

How does a perturbation to a single initial matrix propagate to such large gains?  $S_0$ ’s direct influence on output logits decays to 0.03% KL ratio by the end of the prompt, yet 23 of 27 FAIL-to-PASS flips diverge from the baseline at the very first generated character (85%). The initial perturbation is amplified by the recurrence into a qualitatively different generation trajectory. This is trajectory-steering, distinct from the uniform weight modification that LoRA applies.

## Contributions.

- $S_0$  tuning: a zero-inference-overhead PEFT method that outperforms LoRA by  $+10.8$  pp on GatedDeltaNet (Qwen3.5-4B,  $p < 0.001$ ) and is statistically indistinguishable from LoRA on Mamba-2 in a 3-seed FalconH1 comparison (71.8% vs. 71.4%).
- Parameter-matched control: LoRA at rank 64 (12.6M, equal to  $S_0$ ) degrades by  $-15.5$  pp in this small-data regime, arguing against parameter count alone as the explanation.
- Transformer negative control: prefix tuning on a pure Transformer (Qwen2.5-3B) degrades performance by  $-13.9$  pp under all nine configurations.
- Mechanistic analysis:  $S_0$ ’s direct influence decays to 0.03% KL by the end of the prompt, yet 85% of corrected solutions diverge at the first generated character.
- Scaling and pass@ $k$ : a state-offset variant achieves  $+27.1$  pp; pass@10 reaches 88.5% versus 66.7% for LoRA in a separate 3-seed sampled evaluation.

## 2 Background

### 2.1 Recurrent State Mechanics

In GatedDeltaNet Yang et al. [2024], each recurrent layer maintains a state matrix  $S_t \in \mathbb{R}^{H \times K \times V}$  updated via the gated delta rule:

$$S_t = \alpha_t S_{t-1} (I - \beta_t k_t k_t^\top) + \beta_t v_t k_t^\top, \quad (1)$$

---

**Algorithm 1:**  $S_0$  tuning

---

**Input:** Hybrid model  $f_\theta$ , correct solutions  $\{(x_i, y_i)\}_{i=1}^N$ , scaling  $\alpha$ **Output:** Learned initial states  $\{S_0^{(\ell)}\}_{\ell=1}^L$ 

- 1 Initialize  $S_0^{(\ell)} \leftarrow 0$  for each recurrent layer  $\ell$ ;
  - 2 **for**  $step = 1$  **to**  $T$  **do**
  - 3     Set initial state  $S_0^{(\ell)} \leftarrow \alpha \cdot S_0^{(\ell)}$  for each recurrent layer;
  - 4     Compute loss  $\mathcal{L} = \frac{1}{N} \sum_i \text{CE}(y_i, f_\theta(x_i; \alpha S_0)) + \lambda \sum_\ell \|S_0^{(\ell)}\|_2^2$ ;
  - 5     Update  $S_0^{(\ell)} \leftarrow S_0^{(\ell)} - \eta \nabla_{S_0^{(\ell)}} \mathcal{L}$ ;
  - 6 **return**  $\{S_0^{(\ell)}\}_{\ell=1}^L$ ;
- 

where  $\alpha_t \in (0, 1)$  is a decay gate,  $\beta_t \in (0, 1)$  controls write strength, and  $k_t, v_t$  are key and value vectors. The term  $(I - \beta_t k_t k_t^\top)$  erases the old association for key  $k_t$  before writing the new one. Mamba-2 Dao and Gu [2024] uses a structurally similar update through its structured state-space duality (SSD):

$$S_t = \bar{A}_t S_{t-1} + \bar{B}_t x_t, \quad (2)$$

where  $\bar{A}_t$  is a scalar gate and  $\bar{B}_t$  an input projection. In both architectures, the state is a full matrix: a single GatedDeltaNet layer in Qwen3.5-4B carries  $\sim 524\text{K}$  state entries ( $H=32, K=V=128$ ). Mamba-1 Gu and Dao [2023], by contrast, uses a diagonal state where each of  $N=16$  dimensions evolves independently, with no cross-feature interactions. This structural gap matters. A full matrix state has the capacity to encode cross-feature correlations that a diagonal state lacks, consistent with a state-expressiveness threshold below which initial-state tuning becomes ineffective. By default, both architectures initialize  $S_0 = 0$ ; our method replaces this zero initialization with a learned value.

## 3 Method

### 3.1 $S_0$ Tuning

Hybrid recurrent-attention models expose a recurrent state at every recurrent layer; we treat the initial value of that state as the adaptation surface. For each recurrent layer  $\ell$ , we introduce a learnable tensor  $S_0^{(\ell)}$  with the same shape as the layer’s native recurrent state and freeze all backbone parameters  $\theta$ . Given a prompt-completion pair  $(x, y)$ , the recurrent layer now starts from  $\alpha S_0^{(\ell)}$  rather than the default zero state, where  $\alpha$  is a scalar state-scaling hyperparameter chosen per architecture. We optimize only the collection  $\{S_0^{(\ell)}\}_{\ell=1}^L$  using a completion-only objective,

$$\mathcal{L}(S_0) = \frac{1}{N} \sum_{i=1}^N \text{CE}(y_i^{\text{comp}}, f_\theta(x_i; \alpha S_0)) + \lambda \sum_{\ell=1}^L \|S_0^{(\ell)}\|_2^2,$$

where prompt tokens are masked so gradients act only on the target completion.

1. Initialize  $S_0^{(\ell)} = 0$  for each recurrent layer  $\ell$ .
2. Inject  $S_0^{(\ell)}$  as the initial hidden state before the first token.
3. Optimize  $S_0^{(\ell)}$  via gradient descent on a completion-only loss over correct solutions, with all model weights frozen.
4. At inference,  $S_0$  is absorbed into the recurrent state at  $t = 1$  and adds zero cost at any subsequent timestep.

Qwen3.5 uses  $\alpha = 0.07$ ; FalconH1 uses  $\alpha = 0.65$  (Section 5.7). All other hyperparameters are given in Section 4.4.

We also evaluate a state-offset variant Kang et al. [2025] that adds a learned tensor  $\Delta S^{(\ell)}$  at every timestep (non-zero overhead); see Section 5.5.

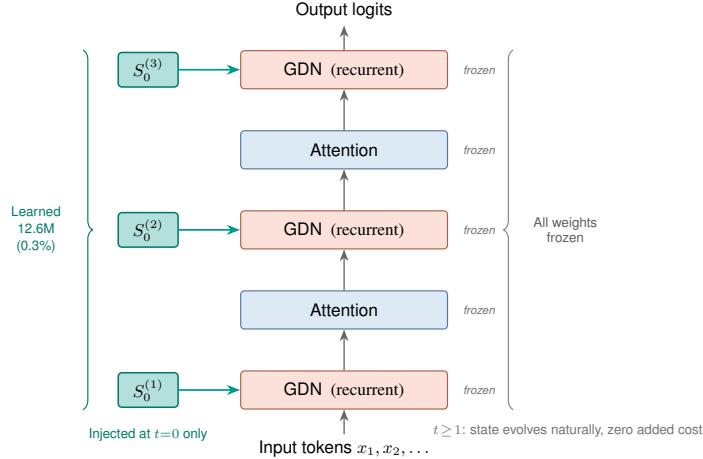


**Figure 2: Computation graph for  $S_0$  tuning.** The learned initial state  $S_0$  (teal) is injected into each recurrent layer before the first token. After  $t=1$ , it is absorbed into the running state and adds zero computational overhead. All model weights remain frozen.

**Zero-overhead property.** Because  $S_0$  is injected only at  $t=0$ , it is absorbed into the running state at  $t=1$ ; every subsequent step executes the unmodified recurrence with no adapter branch and no weight merging.  $S_0$  is therefore zero-inference-overhead as a structural property of the computation graph, not as an empirical approximation.

Figure 2 illustrates the computation graph.

## 4 Experimental Setup

### 4.1 Models

We evaluate on two hybrid architectures. **Qwen3.5-4B** Team [2025b], Yang et al. [2024] interleaves 24 GatedDeltaNet layers with 8 attention layers ( $\sim 3:1$  ratio); each GDN layer carries a state matrix  $S_t \in \mathbb{R}^{32 \times 128 \times 128}$ , totaling 12.6M state parameters (0.3% of the model). **FalconH1-7B** Falcon LLM Team [2025] is a Mamba-2 hybrid where every layer processes tokens through both attention and Mamba-2 heads in parallel, totaling 34.6M state parameters (0.5%). We also evaluate scaling across Qwen3.5- $\{0.8B, 2B, 9B\}$  with identical hyperparameters. All models run in `no_thinking` mode (chain-of-thought generation disabled).

### 4.2 Benchmarks

Our primary benchmark is HumanEval Chen et al. [2021] (164 problems). We reserve problems 0–79 for training data collection and evaluate on the held-out set of problems 80–163 ( $n=84$ ). Training data consists of execution-verified correct solutions sampled from the frozen base model. The main HumanEval pipeline keeps at most one passing completion per train problem, yielding roughly 48 verified solutions total across the 80 training problems. For cross-domain evaluation we test on MATH-500 Hendrycks et al. [2021], GSM8K Cobbe et al. [2021], and Spider Yu et al. [2018] (text-to-SQL) using standard splits.

### 4.3 Baselines

We compare against LoRA Hu et al. [2021] as the primary baseline. On Qwen3.5-4B, LoRA targets  $\{q,k,v,o\}_{proj}$  of the 8 attention layers (rank 24, 4.7M parameters). On FalconH1-7B, LoRA targets  $\{q,k,v,in\}_{proj}$  across all layers (rank 24, 22.2M parameters); `in_proj` belongs to the Mamba-2 mixer, so FalconH1 LoRA adapts *both* attention and recurrent pathways. We select the best of 4 configurations (2 learning rates  $\times$  2 ranks). As a negative control, we apply prefix tuning with matched parameter count to Qwen2.5-3B-Instruct Team [2025a], a pure Transformer (30 virtual tokens, `prefix_projection=True`, 3 learning rates  $\times$  3 seeds). Full configurations are in Appendix A.

**Table 1:** HumanEval main results on held-out problems 80–163. Qwen results use 10 seeds; Falcon results use 3 seeds unless noted otherwise.

Method	Params <sup>†</sup>	Qwen3.5-4B (GatedDeltaNet)	FalconH1-7B (Mamba-2)	Overhead
Baseline	—	48.8%	40.5%	—
LoRA (best config)	4.7M / 22.2M	61.5% ± 5.1%	71.4% ± 2.4%	Merge
State-offset	12.6M / —	74.8% ± 3.6%	—	Per-step
S <sub>0</sub> (ours)	12.6M / 34.6M	<b>72.2% ± 1.7%</b>	<b>71.8% ± 1.3%</b>	None

<sup>†</sup> Params shown as Qwen3.5 / FalconH1. FalconH1 has 44 Mamba-2 layers (vs. 24 GDN layers in Qwen3.5), yielding more state parameters (34.6M vs. 12.6M) and more LoRA targets (22.2M vs. 4.7M). The state-offset accuracy comes from the paired 10-seed run in Table 3: 47.6% baseline + 27.1 pp = 74.7%.

**Comparison caveats.** The primary Qwen comparison uses S<sub>0</sub> at 12.6M versus LoRA rank-24 at 4.7M; Section 5.2 tests matched budgets (rank-64 LoRA degrades by −15.5 pp in the same setup). Unless otherwise noted, Qwen LoRA numbers in the main paper refer to this best rank-24 baseline, while higher-rank LoRA appears only in Section 5.2. S<sub>0</sub> also requires execution-verified solutions, a stronger data assumption than LoRA, and the Falcon comparison remains a supportive 3-seed result rather than a definitive superiority claim.

#### 4.4 Statistical Protocol

All training hyperparameters are in Appendix A. Primary comparisons use 10 random seeds. We report mean ± std and test significance with Welch’s *t*-test (unequal variances). Unless otherwise stated, hypothesis tests in the main paper are two-sided; paired *t*-tests are used only for the dedicated S<sub>0</sub> versus state-offset rerun. Comparisons with only 3 seeds (Falcon, 2B, 9B, and pass@*k*) are reported as supportive evidence rather than headline superiority claims. GPU floating-point non-determinism introduces ~2 pp baseline variation across seeds; this is absorbed into the reported standard deviations.

**Claim hierarchy.** The paper has one anchor claim: on Qwen3.5-4B HumanEval, S<sub>0</sub> beats the main LoRA baseline over 10 seeds. Falcon tests architectural transfer, MATH-500 and GSM8K test domain transfer, Spider marks a failure case, and the matched-budget LoRA plus Transformer prefix-tuning controls test alternative explanations. We use the strongest statistical language only for the comparisons that carry the central claim.

## 5 Results

### 5.1 Main Comparison

Table 1 summarizes the main empirical result. On Qwen3.5-4B, S<sub>0</sub> improves greedy HumanEval pass@1 from 48.8% to 72.2%, a gain of +23.6 ± 1.7 pp over 10 seeds.<sup>1</sup> Against the strongest Qwen LoRA baseline (rank 24), this yields a +10.8 pp advantage (*p* = 0.000056) with roughly 3× lower variance (1.7 vs. 5.1 pp). State-offset attains the highest absolute score on Qwen3.5, but does so by paying a per-step inference cost; S<sub>0</sub> remains the best zero-inference-overhead operating point.

The same table also shows that the result is not specific to one hybrid family. On FalconH1-7B, S<sub>0</sub> reaches 71.8% ± 1.3 with architecture-specific  $\alpha=0.65$ ; LoRA reaches 71.4% ± 2.4. The two methods are statistically indistinguishable at this sample size (3 seeds) while S<sub>0</sub> avoids weight merging and again exhibits lower variance. We treat this as evidence of competitiveness on Falcon rather than a superiority claim.

In a separate 3-seed sampled decoding evaluation, S<sub>0</sub> reaches pass@10 of 88.5% versus 66.7% for LoRA (Table 9 in the appendix), a gap that grows with *k*. LoRA’s pass@5 is tied with the untrained baseline.

<sup>1</sup>Deltas are computed as the mean of per-seed improvements, which may differ slightly from the difference of rounded group means.

**Table 2:** Parameter-matched LoRA comparison on Qwen3.5-4B HumanEval (10 seeds each).

Method	Params	Mean $\Delta$	Std	Seeds negative
LoRA r24	4.7M	+12.7 pp	5.1 pp	0/10
LoRA r48	9.4M	+2.1 pp	17.0 pp	1/10 collapsed
LoRA r64	12.6M	-15.5 pp	18.9 pp	8/10
$S_0$	12.6M	+ <b>23.6</b> pp	1.7 pp	0/10

**Table 3:** State-based comparison on Qwen3.5-4B HumanEval.  $S_0$  and state-offset use a dedicated paired 10-seed rerun; the LoRA row is included only as the main rank-24 reference baseline from Table 1.

Method	Mean $\Delta$	Std	Gap vs. main LoRA	Overhead
LoRA (best)	+12.7 pp	5.1 pp	—	Merge
$S_0$	+23.5 pp	4.0 pp	+10.8 pp	None
State-offset	+27.1 pp	3.6 pp	+14.4 pp	Per-step

## 5.2 Parameter-Matched Comparison

The primary LoRA baseline uses rank 24 (4.7M parameters), roughly one-third of  $S_0$ 's 12.6M. A natural objection is that  $S_0$  wins because it has more capacity. We test this directly by training LoRA at rank 48 (9.4M) and rank 64 (12.6M, exactly matching  $S_0$ ), using the same data, learning rate, and training steps (Table 2).

Increasing LoRA rank makes things worse, not better. Rank 48 averages  $+2.1 \pm 17.0$  pp across 10 seeds, with one catastrophic seed collapsing to 4.8% accuracy. Rank 64, at matched parameter budget, degrades by  $-15.5 \pm 18.9$  pp: 8 of 10 seeds are negative. The pattern is consistent with overfitting in this small-data regime. At matched budget, the gap between  $S_0$  (+23.6 pp) and LoRA rank-64 (-15.5 pp) is 39 pp: identical parameter counts organized as recurrent states versus weight matrices produce opposite outcomes in this setting.

## 5.3 Cross-Architecture Transfer

Qwen3.5 (interleaved GatedDeltaNet + attention) and FalconH1-7B (parallel Mamba-2 + attention) differ in both recurrence family and hybrid topology, making the cross-architecture result a stronger test. The Falcon result in Table 1 shows  $S_0$  remains competitive even when LoRA targets the Mamba-2 `in_proj` pathway, but we regard this as supportive evidence until a larger-seed replication is run.

## 5.4 Scaling Behavior

Figure 3(a) shows a strong scale trend within the Qwen3.5 family. The 0.8B model exhibits only a directional gain ( $+2.6 \pm 3.7$  pp,  $p=0.076$ ), but performance improves sharply at 2B ( $+19.0 \pm 1.2$  pp,  $p=0.001$ ), 4B ( $+23.6 \pm 1.7$  pp), and 9B ( $+44.0 \pm 1.2$  pp,  $p=0.0002$ ). Gains increase with model scale, from +2.6 pp at 0.8B to +44.0 pp at 9B, though the non-monotonic baseline complicates scaling analysis. The 9B baseline (32.1%) is lower than the 4B (48.8%) because suppressing chain-of-thought degrades the larger model more;  $S_0$  recovers it to 76.1%. Full scaling data are in Appendix H.

## 5.5 State-Offset Comparison

A per-step state-offset variant Kang et al. [2025] achieves +27.1 pp (Table 3), the strongest absolute accuracy, but at per-step inference cost. Table 3 uses a dedicated paired rerun for the two state-based methods, which is why  $S_0$  appears there as  $+23.5 \pm 4.0$  pp rather than the main-run  $+23.6 \pm 1.7$  pp. In that paired rerun,  $S_0$  captures 87% of the offset's gain (+23.5 of +27.1 pp) at zero runtime cost. The paired rerun is only for comparing  $S_0$  with state-offset; LoRA is shown in Table 3 as the main rank-24 reference baseline from Table 1.

## 5.6 Cross-Domain Transfer

Cross-domain gains are smaller but statistically significant: MATH-500 improves by  $+4.8 \pm 1.4$  pp (two-sided  $p=0.00002$ , 8 seeds) and GSM8K by  $+2.8 \pm 1.6$  pp (two-sided  $p=0.0003$ , 10 seeds).

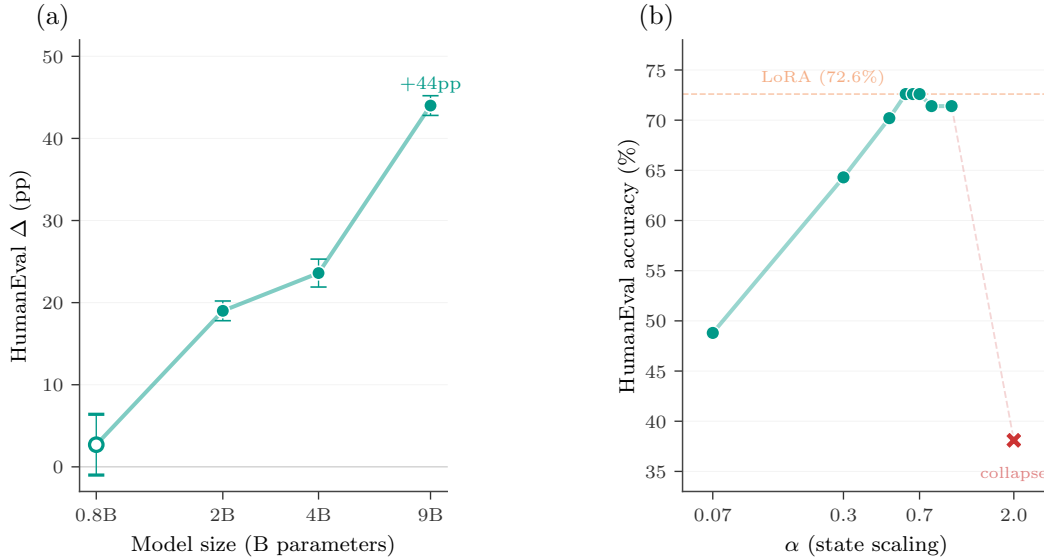


**Figure 3: Scaling and architecture-specific tuning.** (a) Performance gains increase monotonically with model scale, from +2.6 pp at 0.8B to +44.0 pp at 9B. Error bars show  $\pm 1$  standard deviation across seeds. The 9B model achieves 76.1% absolute accuracy from a 32.1% baseline, suggesting larger models have more latent capability to unlock via state initialization. (b) FalconH1 alpha sweep: the default  $\alpha=0.07$  yields only +8.3 pp, but architecture-specific tuning to  $\alpha=0.6$ –0.7 reaches 71.8%, matching LoRA’s 71.4%. Large  $\alpha$  ( $\geq 2.0$ ) collapses performance.

Spider text-to-SQL shows no transfer (+0.0 pp across five alpha values in a single-seed alpha sweep), consistent with the trajectory-steering mechanism: SQL queries have low early-token diversity, so the initial-state perturbation has little to steer. We treat Spider as a boundary-condition observation rather than a formal significance result.

### 5.7 Architecture-Specific Alpha

The alpha sweep (Appendix E) explains why the first Falcon result understated the method’s potential. The Qwen-optimal default  $\alpha=0.07$  improves FalconH1 by only +8.3 pp, but performance rises steeply as the scale increases, plateauing at 0.60–0.70 at 71.8% accuracy, matching LoRA’s 71.4%. Pushing  $\alpha$  too far eventually collapses the model: at  $\alpha=2.0$ , accuracy falls below the baseline.

Full alpha sweep values are in Appendix E.

### 5.8 Transformer Negative Control

Prefix tuning on a pure Transformer (Qwen2.5-3B) degrades performance by  $-13.9$  pp (all 9 configurations negative, 95% CI upper bound  $-5.3\%$ ); the gap to hybrid  $S_0$  is +37.5 pp, consistent with recurrence playing a key role.

## 6 Mechanistic Analysis

$S_0$  tuning produces large accuracy gains on two hybrid architectures while matched-parameter prefix tuning on a pure Transformer fails entirely ( $-13.9$  pp). *Why* does tuning the recurrent initial state succeed where prefix tuning does not? We examine persistence analysis, first-character divergence, linear probing, and architecture-specific gating dynamics.

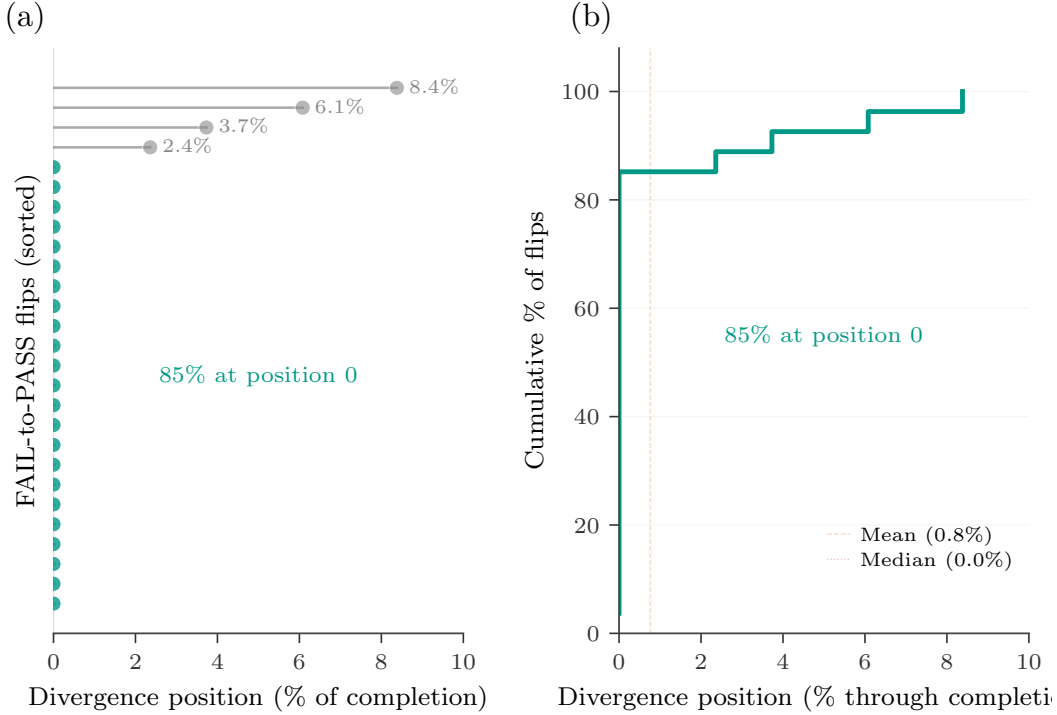


**Figure 4: First-character divergence in FAIL-to-PASS flips** (27 flips, single-seed Qwen3.5-4B). (a) 23 of 27 corrected solutions (85%) diverge from baseline at character position 0, the very first generated character. (b) Cumulative distribution of divergence positions: all 27 flips diverge within the first 10% of the completion (mean 0.76%, median 0.0%).  $S_0$  shifts the output distribution at the first opportunity; autoregressive decoding amplifies this into a qualitatively different solution.

## 6.1 The Launch Vector Effect

Consider the GatedDeltaNet update (Eq. 1) applied over  $T$  prompt tokens.  $S_0$ 's contribution to the state at position  $T$  is

$$S_T^{(S_0)} = S_0 \prod_{t=1}^T G_t, \quad G_t = \alpha_t (I - \beta_t k_t k_t^\top), \quad (3)$$

where each  $G_t$  is the per-step gating matrix. When the decay gates  $\alpha_t$  are close to 1 and the write strengths  $\beta_t$  are small, the product  $\prod G_t$  retains a nonzero component of  $S_0$ ; when gating is aggressive,  $S_0$  decays toward zero. This yields two testable predictions: the direct KL influence of  $S_0$  on output logits should decay roughly exponentially through the prompt, at a rate set by the average gate magnitude, and architectures with different gating statistics (GDN vs. Mamba-2) should require proportionally different alpha scaling to achieve the same effective perturbation, explaining the  $10\times$  gap between optimal alpha values. We test both below.

## 6.2 Persistence Analysis

Equation 3 predicts exponential decay of  $S_0$ 's direct influence. We test this by comparing forward passes with the tuned state against forward passes with the default zero state, both conditioned on the same prompt tokens. We measure the KL divergence ratio between the two output distributions at each position. The influence decays through the prompt context, reaching 0.03% by the final prompt token, matching the predicted exponential profile. By the time generation begins, the tuned state and zero state produce almost identical next-token distributions *over the prompt*. The signal has not vanished. It has been absorbed into the recurrent state as a low-magnitude directional bias: a slight but consistent skew in the hidden representation rather than a large perturbation to the output logits.

### 6.3 First-Character Divergence

If  $S_0$  acts as a soft prompt in recurrent memory, its effect should be visible the moment the model begins generating. We test this by examining all 27 FAIL-to-PASS flips from a single-seed Qwen3.5-4B evaluation and recording the first character position at which the tuned and baseline greedy outputs differ. Of these 27 flips, 23 (85%) diverge at character position 0, the very first generated character. The remaining 4 diverge at positions 16, 28, 32, and 36; all 27 diverge within the first 10% of the completion. A sign test for concentration within the first 10% yields  $p < 10^{-8}$ .  $S_0$  does not gradually steer generation over many tokens. It shifts the model’s output distribution at the first opportunity, and autoregressive decoding amplifies that initial divergence into a qualitatively different solution. This is exactly what the persistence analysis predicts: by the time generation begins,  $S_0$  has been compressed into the recurrent state as a small directional bias that is just large enough to flip the argmax at the first generated character.

### 6.4 Architecture-Specific Gating and Probing

Equation 3 also predicts that architectures with different gating statistics can require different alpha scaling. GDN layers in Qwen3.5 use both a scalar decay  $\alpha_t$  and a key-dependent erasure term  $\beta_t k_t k_t^\top$ , whereas Mamba-2 layers in FalconH1 use scalar gating through SSD. The observed  $10\times$  gap (0.07 for Qwen3.5 vs. 0.65 for FalconH1; Appendix E) shows that the same initial-state scale does not transfer unchanged across recurrence families. A linear probe trained to predict solution correctness from intermediate representations (PCA-reduced to 64 dimensions; see Appendix H for full protocol) achieves AUC = 0.93 when reading from the recurrent state versus AUC = 0.90 from the residual stream. This 2.5-point gap (0.930 vs. 0.905) is descriptive rather than inferential, but it suggests that the recurrent state encodes task-relevant information at least as directly as the residual stream.

## 7 Related Work

### 7.1 PEFT for State Space Models

The PEFT literature for SSMs shares a common finding: on diagonal-state architectures, LoRA wins. Galim et al. [2024] showed this most directly at ICML 2025, comparing LoRA against initial-state tuning on Mamba-1 (their appendix extends to Jamba and Mamba-II with scalar or small-dimensional states). MambaPEFT Yoshimura et al. [2024] evaluated 20 PEFT variants without testing initial-state tuning at all. ProDial Ham et al. [2024] and SSMLoRA Yu et al. [2025] explored projector and hybrid adaptations; Memba Lee et al. [2025] introduced membrane gating. None of these works tested matrix-valued states. Prefix tuning Li and Liang [2021] prepends learnable key-value vectors to Transformer attention; we use it as a negative control (Section 5.8).

On GatedDeltaNet and Mamba-2, where states are full matrices ( $\sim 524\text{K}$  entries per layer), we observe the opposite:  $S_0$  tuning outperforms LoRA by +10.8 pp ( $p < 0.001$ ) on Qwen3.5. The reversal supports a state-expressiveness hypothesis: a 524K-entry matrix can encode enough task-relevant structure for PEFT, while a diagonal state does not appear to.

### 7.2 State-Based Adaptation

State-offset tuning Kang et al. [2025] adds a per-step learned offset to Mamba-1 hidden states (up to 1.4B parameters, NLU benchmarks). Liu et al. [2025] tune RWKV-7 states with kernel upscaling and decorrelated backpropagation, framed as test-time scaling rather than PEFT; we adopt the name  $S_0$  tuning to distinguish our gradient-based approach from their broader “State Tuning” framework. Lina-Speech Lemerle et al. [2024] optimizes  $S_0$  of Gated Linear Attention layers for TTS voice cloning, the closest prior art to our mechanism but in a different domain and without LoRA comparison.

Independent work establishes that recurrent states *encode* task identity even without optimization. State Soup Pióro et al. [2024] showed that in-context-learned states in Mamba-2.8B cluster by task and that interpolating them improves few-shot performance. We go further: instead of interpolating states that arise from in-context learning, we optimize them directly via gradient descent.

We extend the offset idea to GatedDeltaNet, where our offset variant reaches +27.1 pp (beating LoRA at  $p < 0.001$ ); the pure- $S_0$  variant trades peak accuracy for zero inference overhead. No prior work validates state-based PEFT across multiple recurrence families in a single study.

### 7.3 Hybrid Architectures

Mamba-2 Dao and Gu [2024] introduced structured state space duality with matrix-valued states; GatedDeltaNet Yang et al. [2024] applied the delta rule to linear attention. Qwen3.5 interleaves GatedDeltaNet layers with standard attention at a roughly 3:1 ratio; FalconH1 Falcon LLM Team [2025] places Mamba-2 and attention heads in parallel within every layer. Mamba-3 Lahoti et al. [2026] and Wang et al. [2025] study how to design and analyze such hybrids. The recurrent state ( $S_t \in \mathbb{R}^{H \times K \times V}$ , updated at every token) is the adaptation surface our method targets;  $S_0$  tuning tunes it while leaving all weights frozen.

## 8 Discussion and Limitations

**Code-math gap.**  $S_0$  tuning is strongest on code generation (+23.6 pp on HumanEval). Cross-domain transfer to MATH-500 (+4.8 pp, two-sided  $p=0.00002$ , 8 seeds) and GSM8K (+2.8 pp, two-sided  $p=0.0003$ , 10 seeds) is statistically significant but substantially smaller. Spider text-to-SQL (+0.0 pp) shows no transfer to structured-output tasks.

**Diagonal vs. matrix states.** Our results are on architectures with matrix-valued states (GatedDeltaNet, Mamba-2). Galim et al. [2024] showed that initial-state tuning underperforms LoRA on diagonal-state Mamba-1, consistent with a state-expressiveness threshold below which initial-state tuning cannot compete with weight adaptation.

**Training data.**  $S_0$  tuning requires execution-verified correct solutions ( $\sim 48$  verified completions for our HumanEval setup). That is a small training set relative to the breadth of our claims, so the headline result should be read as small-data evidence that recurrent state is a strong adaptation surface in this regime. Applying  $S_0$  where verification is expensive remains untested. LoRA imposes no such constraint. HumanEval problems may appear in pretraining data; cross-domain gains on MATH-500 and GSM8K argue against a memorization-only explanation, and the null result on Spider further bounds the scope of transfer. Training takes 3 minutes on a single A10G GPU; as few as 25 solutions suffice for stable gains (Appendix D).

**Evidence strength and compute budget.** The core result is overdetermined on Qwen. The thinner comparisons serve a different job: Falcon checks architectural transfer, Spider marks a failure mode, and the auxiliary sweeps show how far the effect moves beyond the anchor setting. Falcon still uses 3 seeds, Spider is a single-seed alpha sweep, and we did not keep broadening the benchmark grid once the project hit a fixed personal GPU budget rather than institutional cluster access. We therefore present these experiments as transfer checks and boundary conditions, not as a complete benchmark sweep over every competing method and category.

## 9 Conclusion

$S_0$  tuning optimizes only the initial recurrent state of hybrid language models, adding zero inference overhead. On Qwen3.5-4B,  $S_0$  outperforms LoRA by +10.8 pp ( $p < 0.001$ ); on FalconH1-7B it is statistically indistinguishable from LoRA in a 3-seed comparison (71.8% vs. 71.4%). A prefix-tuning control on a pure Transformer fails under all configurations. Cross-domain transfer to MATH-500 and GSM8K is significant ( $p < 0.001$ ), though the method does not transfer to structured-output SQL. Matrix-valued recurrent states Galim et al. [2024] appear to provide an expressive adaptation surface that LoRA leaves unused in this setting;  $S_0$  is a competitive zero-inference-overhead PEFT method for exploiting it.

## References

Mark Chen et al. Evaluating large language models trained on code. *arXiv preprint arXiv:2107.03374*, 2021.

- Karl Cobbe, Vinod Kosaraju, Mohammad Bavarian, Mark Chen, Heewoo Jun, Lukasz Kaiser, Matthias Plappert, Jerry Tworek, Jacob Hilton, Reiichiro Nakano, Christopher Hesse, and John Schulman. Training verifiers to solve math word problems. *arXiv preprint arXiv:2110.14168*, 2021.
- Tri Dao and Albert Gu. Transformers are SSMs: Generalized models and efficient algorithms through structured state space duality. *arXiv preprint arXiv:2405.21060*, 2024.
- Falcon LLM Team. Falcon-H1: A family of hybrid-head language models redefining efficiency and performance. *arXiv preprint arXiv:2507.22448*, 2025.
- Tristan Galim, Adrien Bénédict, Amir Moawad, Romain Franceschini, and Edouard Mathieu. Parameter-efficient fine-tuning of state space models. *arXiv preprint arXiv:2410.09016*, 2024. ICML 2025.
- Albert Gu and Tri Dao. Mamba: Linear-time sequence modeling with selective state spaces. *arXiv preprint arXiv:2312.00752*, 2023.
- Seokil Ham, Hee-Seon Kim, Sangmin Woo, and Changick Kim. Parameter efficient mamba tuning via projector-targeted diagonal-centric linear transformation. *arXiv preprint arXiv:2411.15224*, 2024.
- Dan Hendrycks, Collin Burns, Saurav Kadavath, Akul Arora, Steven Basart, Eric Tang, Dawn Song, and Jacob Steinhardt. MATH: Measuring mathematical problem solving with the MATH dataset. *arXiv preprint arXiv:2103.03874*, 2021. NeurIPS 2021.
- Edward J. Hu, Yelong Shen, Phillip Wallis, Zeyuan Allen-Zhu, Yuanzhi Li, Shean Wang, Lu Wang, and Weizhu Chen. LoRA: Low-rank adaptation of large language models. *arXiv preprint arXiv:2106.09685*, 2021. ICLR 2022.
- Wonjun Kang, Kevin Galim, Yuchen Zeng, Minjae Lee, Hyung Il Koo, and Nam Ik Cho. State-offset tuning: State-based parameter-efficient fine-tuning for state space models. *arXiv preprint arXiv:2503.03499*, 2025. ACL 2025.
- Aakash Lahoti, Kevin Y. Li, Berlin Chen, Caitlin Wang, Aviv Bick, J. Zico Kolter, Tri Dao, and Albert Gu. Mamba-3: Improved sequence modeling using state space principles. *arXiv preprint arXiv:2603.15569*, 2026. ICLR 2026.
- Donghyun Lee, Yuhang Li, Ruokai Yin, Shiting Xiao, and Priyadarshini Panda. Memba: Membrane-driven parameter-efficient fine-tuning for mamba. *arXiv preprint arXiv:2506.18184*, 2025.
- Théodore Lemerle, Adel Music, Nicolas Music, and Thomas Music. Lina-Speech: Gated linear attention is a fast and parameter-efficient learner for text-to-speech synthesis. *arXiv preprint arXiv:2410.23320*, 2024.
- Xiang Lisa Li and Percy Liang. Prefix-tuning: Optimizing continuous prompts for generation. In *Proceedings of the 59th Annual Meeting of the Association for Computational Linguistics*, 2021.
- Xiao Liu et al. State tuning: Tuning the recurrent state for efficient adaptation of large language models. *arXiv preprint arXiv:2504.05097*, 2025.
- Maciej Pióro et al. State soup: In-context skill learning, retrieval and mixing. *arXiv preprint arXiv:2406.08423*, 2024.
- Qwen Team. Qwen2.5 technical report. *arXiv preprint arXiv:2412.15115*, 2025a.
- Qwen Team. Qwen3 technical report. *arXiv preprint arXiv:2505.09388*, 2025b.
- Dustin Wang, Rui-Jie Zhu, Steven Abreu, Yong Shan, Taylor Kergan, Yuqi Pan, Yuhong Chou, Zheng Li, Ge Zhang, Wenhao Huang, and Jason Eshraghian. A systematic analysis of hybrid linear attention. *arXiv preprint arXiv:2507.06457*, 2025.
- Songlin Yang, Jan Kautz, and Ali Hatamizadeh. Gated delta networks: Improving mamba2 with delta rule. *arXiv preprint arXiv:2412.06464*, 2024. ICLR 2025.

Masakazu Yoshimura, Teruaki Hayashi, and Yota Maeda. MambaPEFT: Exploring parameter-efficient fine-tuning for mamba. *arXiv preprint arXiv:2411.03855*, 2024.

Jiayang Yu, Yihang Zhang, Bin Wang, Peiqin Lin, Yongkang Liu, and Shi Feng. SSMLoRA: Enhancing low-rank adaptation with state space model. *arXiv preprint arXiv:2502.04958*, 2025.

Tao Yu, Rui Zhang, Kai Yang, Michihiro Yasunaga, Dongxu Wang, Zifan Li, James Ma, Irene Li, Qingning Yao, Shanelle Roman, Zilin Zhang, and Dragomir Radev. Spider: A large-scale human-labeled dataset for complex and cross-database semantic parsing and text-to-sql task. In *EMNLP*, 2018.

## A Hyperparameters

Table 4 lists all hyperparameters for the  $S_0$  and LoRA experiments reported in the main text.

**Table 4:** Hyperparameters for the Qwen3.5 and FalconH1 experiments.

Hyperparameter	$S_0$	LoRA
Learning rate	$1 \times 10^{-3}$	$5 \times 10^{-4}$ (Qwen) / $1 \times 10^{-4}$ (Falcon)
Optimizer	Adam	Adam
Training steps	20	50
Batch size	1	1
L2 regularization	$5 \times 10^{-4}$	—
Alpha scaling	0.07 (GDN) / 0.65 (Mamba-2)	—
LoRA rank	—	24 (primary) / 48, 64 (matched-budget)
LoRA target	—	{q,k,v,o}_proj (Qwen) / {q,k,v,in}_proj (Falcon) <sup>‡</sup>
Loss	Completion-only	Completion-only
Training data	Correct HumanEval train solutions	Correct HumanEval train solutions
Precision	bf16	bf16
Hardware	NVIDIA A10G (24 GB)	NVIDIA A10G (24 GB)
Training time	~3 min	~5 min
Trainable params	12.6M (Qwen) / 34.6M (Falcon) <sup>†</sup>	4.7M (Qwen) / 22.2M (Falcon)

<sup>‡</sup> On FalconH1-7B, `in_proj` belongs to the Mamba-2 mixer, so the Falcon LoRA baseline adapts both attention and recurrent pathways.

<sup>†</sup> On FalconH1-7B,  $S_0$  tunes 34.6M parameters (0.5%) due to larger Mamba-2 state matrices.

## B Layer Sensitivity Ablation

Table 5 breaks down the contribution of each layer group. The ordering early > middle > late is consistent, with gaps of approximately 5 pp between adjacent groups ( $\sim 3\sigma$  separation). Early layers (0–7) alone recover +23.8 pp, matching the full-model +22.6 pp at one-third the parameter count (4.2M vs. 12.6M). Late layers yield the smallest gain (+13.1 pp) but produce zero degradations, making them the safest choice under a strict “do no harm” constraint. If parameter budget is the binding concern, tuning only the first 8 layers is a practical default.

**Table 5:** Layer sensitivity ablation on Qwen3.5-4B HumanEval (single seed).

Layers Tuned	# Layers	Greedy $\Delta$	Degraded	Params
Early (0–7)	8	+23.8 pp	2	4.2M
Middle (8–15)	8	+19.0 pp	3	4.2M
Late (16–23)	8	+13.1 pp	0	4.2M
All (0–23)	24	+22.6 pp	4	12.6M

## C Per-Seed Results

Tables 6 and 7 report per-seed results for full reproducibility.

**Table 6:** Per-seed LoRA results on Qwen3.5-4B HumanEval (best configuration:  $lr = 5 \times 10^{-4}$ , rank 24, 50 steps).

Seed	LoRA $\Delta$	Degraded
42	+9.5 pp	0
7	+17.9 pp	0
123	+20.2 pp	0
1337	+15.5 pp	10
999	+17.9 pp	6
314	+11.9 pp	11
256	+8.3 pp	12
777	+3.6 pp	14
555	+10.7 pp	7
2024	+11.9 pp	7
<b>Mean</b>	$+12.7 \pm 5.1$ pp	—

**Table 7:** FalconH1-7B per-seed results at  $\alpha=0.65$  on HumanEval held-out problems 80–163.

Seed	Baseline	Tuned	$\Delta$	Degraded
42	40.5%	72.6%	+32.1 pp	—
7	40.5%	70.2%	+29.8 pp	—
123	40.5%	72.6%	+32.1 pp	—
<b>Mean</b>	40.5%	71.8%	$+31.3 \pm 1.3$ pp	—

## D Training Data Efficiency

We vary the number of correct training solutions used to optimize  $S_0$  (3 seeds each, Qwen3.5-4B, HumanEval). With only 10 solutions, the method already produces a  $+25.4 \pm 6.8$  pp gain, though variance is high. At 25 solutions the mean stabilizes to  $+22.6 \pm 3.2$  pp, and doubling to 50 solutions yields the same mean ( $+22.6$  pp) with no further benefit. The method is data-efficient: 25 correct solutions suffice for stable gains, and even 10 are enough to see large (if noisy) improvements. Practitioners with limited labeled data can expect usable results from a small pool of verified solutions.

## E Alpha Sweep

On Qwen3.5-4B (GatedDeltaNet), we sweep the alpha scaling factor using a sampled metric (temperature 0.7, single seed). Performance plateaus across a wide range:  $\alpha=0.03$  through  $\alpha=0.15$  all yield  $+30$ – $+34$  pp sampled gains, with the peak at  $\alpha=0.07$  ( $+33.9$  pp sampled). These sampled numbers are higher than the greedy 10-seed mean of  $+23.6$  pp reported in the main text because sampling at temperature 0.7 amplifies the effect of the learned prior. The broad plateau means the method is not sensitive to alpha within this range on GatedDeltaNet.

The FalconH1-7B sweep tells a different story. Applying the GatedDeltaNet-optimal  $\alpha=0.07$  to Mamba-2 yields only  $+8.3$  pp, while the optimal range of  $\alpha=0.60$ – $0.70$  reaches 71.8% accuracy, a  $4\times$  larger gain. The roughly  $10\times$  scale difference between the two architectures (0.07 vs. 0.65) shows that the effective state scale is architecture-specific. GatedDeltaNet combines scalar decay with key-dependent erasure, while Mamba-2 uses SSD gating; our experiments do not isolate which part of the update drives the alpha shift, only that transferring the Qwen setting unchanged leaves a large amount of Falcon performance on the table. Architecture-specific alpha calibration is therefore necessary when transferring  $S_0$  tuning to a new recurrent backbone.

## F Parameter-Matched LoRA Per-Seed Results

Table 8 reports per-seed results for the higher-rank LoRA experiments. At rank 48, one seed (555) collapses to 4.8% accuracy; excluding this outlier, the mean is  $+7.3 \pm 5.5$  pp, still far below  $S_0$ 's  $+23.6 \pm 1.7$  pp. At rank 64 (matched to  $S_0$ 's 12.6M parameters), 8 of 10 seeds are negative, with

deltas ranging from  $-41.7$  pp to  $+13.1$  pp. All configurations use identical training data, learning rate ( $5 \times 10^{-4}$ ), and steps (50); `lora_alpha` is set to  $2r$  following standard practice.

**Table 8:** Per-seed results for higher-rank LoRA on Qwen3.5-4B HumanEval.  
**Rank 48 (9.4M)** **Rank 64 (12.6M, matched)**

Seed	$\Delta$	Note	Seed	$\Delta$
42	+6.0 pp		42	-4.8 pp
7	+10.7 pp		7	-33.3 pp
123	+0.0 pp		123	-29.8 pp
256	+11.9 pp		256	-41.7 pp
999	+3.6 pp		999	+10.7 pp
314	+2.4 pp		314	-19.0 pp
555	-44.0 pp	Collapsed	555	-6.0 pp
777	+3.6 pp		777	-32.1 pp
1337	+10.7 pp		1337	-11.9 pp
2024	+16.7 pp		2024	+13.1 pp
<b>Mean</b>	$+2.1 \pm 17.0$ pp			<b>Mean</b>

## G pass@k Results

Table 9 reports aggregate pass@k results.

**Table 9:** HumanEval pass@k results on held-out problems 80–163 (3 seeds).

Method	pass@1	pass@5	pass@10
Baseline	41.9%	64.2%	69.4%
LoRA (r24, 4.7M)	56.3%	64.1%	66.7%
S <sub>0</sub> (12.6M)	<b>70.3%</b>	<b>84.5%</b>	<b>88.5%</b>

### G.1 Per-Seed Results

Table 10 reports per-seed pass@k estimates for all three methods (3 seeds each). S<sub>0</sub> exhibits low variance across seeds at every k, while LoRA’s pass@5 and pass@10 are within noise of the baseline.

**Table 10:** Per-seed HumanEval pass@k results on held-out problems 80–163.

Method	Seed	pass@1	pass@5	pass@10
Baseline	7	42.1%	63.6%	69.0%
	42	43.5%	64.6%	70.2%
	123	40.1%	64.3%	69.0%
LoRA r24	7	56.4%	63.4%	65.5%
	42	56.4%	64.7%	67.9%
	123	56.0%	64.1%	66.7%
S <sub>0</sub>	7	69.6%	83.8%	86.9%
	42	72.6%	86.4%	90.5%
	123	68.6%	83.3%	88.1%

## H Probing Protocol and Scaling Data

We probe whether the recurrent state encodes task-relevant information more strongly than the residual stream. For each HumanEval problem, we extract the recurrent state  $S_t$  from every GatedDeltaNet layer and the residual-stream hidden state, both at the final prompt token, projected to 64 dimensions via PCA (fit on train split only). A logistic regression probe with 5-fold CV achieves AUC = 0.93 from the recurrent state (best layer: 18) versus AUC = 0.90 from the residual stream (best layer: 23).

The 2.5-point gap is directional evidence that recurrent states encode task-relevant information at least as strongly as residual-stream activations.

**Scaling data.** HumanEval results across Qwen3.5 model sizes. The 0.8B result is borderline ( $p=0.076$ ); at 4B and above, gains are large and unambiguous.

Model	GDN	State	Base	Tuned	$\Delta$
Qwen3.5-0.8B	18	4.7M	14.3%	16.9%	+2.6 $\pm$ 3.7 pp
Qwen3.5-2B	18	4.7M	16.7%	35.7%	+19.0 $\pm$ 1.2 pp
Qwen3.5-4B	24	12.6M	48.8%	72.2%	+23.6 $\pm$ 1.7 pp
Qwen3.5-9B	24	12.6M	32.1%	76.1%	+44.0 $\pm$ 1.2 pp